
From Projection to Prediction: Beyond Logits for Scalable Language Models

Jianbing Dong[†]

NVIDIA

jianbingd@nvidia.com

Jianbin Chang

NVIDIA

jianbinc@nvidia.com

Abstract

Training Large Language Models (LLMs) typically involves a two-stage pipeline at the output layer: hidden states are projected into vocabulary logits via a linear transformation (`lm_head`), followed by cross-entropy loss computation against target tokens. While conceptually simple, this design incurs substantial overhead. The intermediate logits tensor, with dimensions proportional to batch size, sequence length, and vocabulary size, must be fully materialized in GPU memory, even though only one target token per position is ultimately used. This leads to significant memory footprint and bandwidth consumption, limiting scalability and slowing training throughput.

In this work, we introduce a novel approach to integrates the output projection and loss prediction into a single operation. By directly computing the loss from hidden states and target tokens, our approach bypasses explicit logits materialization. This design reduces memory usage and alleviates bandwidth pressure. Experiments on LLM training demonstrate that our method achieves substantial memory savings and measurable speedups compared to the standard two-stage pipeline, enabling large batch sizes and longer sequences without sacrificing accuracy. Our work highlights the benefits of rethinking the boundary between projection and prediction, offering a practical systems optimization for efficient LLM training.

Keywords: LLM, Output Projection, Cross-Entropy Loss, Memory Footprint Reduction

1 Introduction

LARGE language models (LLMs) have rapidly advanced the state of natural language processing, powering applications in dialogue systems [1, 2], code generation [3], and scientific discovery [4]. Their success has been enabled by scaling both model size and training data, but this scaling comes at a steep computational and memory cost [5–7]. As models grow to billions

[†]Corresponding author

of parameters and vocabularies reach hundreds of thousands of tokens, even seemingly routine components of the training pipeline can become critical bottlenecks [8].

A particularly important bottleneck lies in the output layer. In every standard LLM training workflow, hidden states are projected into vocabulary logits through a large linear transformation known as the `lm_head`. These logits are then consumed by a cross-entropy loss function to predict target tokens. This two-stage design is not an implementation detail but a canonical requirement: the `lm_head` projection and cross-entropy loss together define how probability distributions over vocabularies are learned [9]. However, prevailing implementations invariably insist on materializing the entire logits tensor in GPU memory [10], a practice that inflates computational overhead and saturates bandwidth despite its limited utility. The tensor’s dimensions scale with batch size, sequence length, and vocabulary size, leading to substantial memory footprint and bandwidth consumption. Crucially, only one target logit per position is ultimately used in the numerator of the loss, meaning the vast majority of the computed logits are discarded. This mismatch between computation and utility limits scalability and slows training throughput.

Recent research has explored kernel fusion and operator optimization in other parts of the LLM training stack, such as online softmax [11], attention mechanisms [12, 13], and optimizer updates [14, 15]. These efforts highlight the importance of reducing redundant memory movement and improving arithmetic intensity. To the best of our knowledge, the output projection and loss computation — despite being a mandatory stage in every LLM pipeline — have remained largely untouched [9]. Existing frameworks continue to treat the `lm_head` and cross-entropy loss as separate modules, leaving untapped opportunities for optimization.

In this work, we propose a fused kernel implementation that integrates the output projection and loss prediction into a single operation. By directly computing the loss from hidden states and target tokens, our approach bypasses explicit logits materialization while preserving the standard training semantics. This design reduces memory usage, alleviates bandwidth pressure, and improves throughput. Experiments on LLM training demonstrate that our method achieves substantial memory savings and measurable speedups compared to the canonical two-stage pipeline, enabling larger batch sizes and longer sequences without sacrificing accuracy.

Our contributions underscore the value of rethinking the boundary between projection and prediction. By collapsing these stages into a unified kernel, we provide a practical systems optimization that addresses a critical bottleneck in the universally adopted LLM training workflow. Beyond immediate performance gains, this work contributes to the broader effort of making large-scale language modeling more efficient, sustainable, and accessible.

2 Related Work

Optimizing the efficiency of large language model training has been a central focus of recent systems research. A recurring theme is the reduction of redundant memory movement and the fusion of operations to improve arithmetic intensity [16]. These efforts demonstrate that even small changes to core primitives can yield substantial performance gains at scale.

2.1 Softmax Optimizations

Online Softmax [11] introduced a memory-efficient reformulation of the softmax operator that reduces redundant memory accesses by computing the normalization term in a single pass over the input vector. This approach improves GPU performance for bandwidth-bound workloads,

achieving up to $1.3\times$ speedup compared to the standard safe softmax implementation. Furthermore, by fusing Online Softmax with the commonly used Top-K operation in beam search, they demonstrated up to $5\times$ performance gains. This work highlights how kernel-level optimizations in seemingly routine components of the training stack can deliver substantial efficiency improvements, influencing subsequent research on operator fusion and memory-aware kernel design in LLM systems.

2.2 Attention Mechanism Optimizations

The attention mechanism has been another major target for kernel fusion. FlashAttention [12, 13] introduced a highly optimized, IO-aware algorithm that computes attention in a tiled fashion, thereby avoiding the materialization of large intermediate matrices. By tightly coordinating memory access with computation, FlashAttention achieves significant speedups and memory savings, enabling training with longer sequence lengths and larger batch sizes. This line of work illustrates how re-engineering core components of the transformer architecture [17] can unlock substantial efficiency gains and expand the practical limits of large-scale model training.

2.3 Operator Fusion in LLM Systems

Operator fusion has also been widely adopted in industry-grade libraries. NVIDIA’s TransformerEngine [18] provides a suite of fused CUDA kernels tailored for transformer workloads [17], including GEMM combined with bias addition and activation functions, fused layer normalization, and optimized softmax variants. By collapsing multiple sequential operations into a single kernel, TransformerEngine eliminates redundant memory movement and reduces kernel launch overhead, thereby improving arithmetic intensity and throughput. These fused primitives are designed to exploit Tensor Cores and mixed-precision formats such as FP8 and BF16, enabling efficient training and inference of very large language models. TransformerEngine exemplifies how production systems integrate operator fusion into the transformer stack, complementing research efforts like Online Softmax and FlashAttention, and reinforcing the broader trend of re-engineering fundamental components for efficiency.

Together, these efforts highlight a broader trajectory: efficiency gains in LLM training often arise from collapsing boundaries between traditionally separate operations. In line with this trajectory, we introduce a kernel-level optimization that pushes forward the broader agenda of reducing memory movement and improving arithmetic intensity in LLM systems.

3 Methodology

3.1 Standard Output Projection and Loss Prediction

In conventional LLM training, the output layer consists of two sequential operations:

- a) Projection into vocabulary logits

Given hidden states $H \in R^{B \times T \times d}$ and $W \in R^{V \times d}$, where B is the batch size, T is the sequence length, d is the hidden dimension, and V is the vocabulary size, the logits are computed as:

$$Z = H \cdot W^T \tag{1}$$

where \cdot denotes the matrix multiplication. $Z \in R^{B \times T \times V}$ is the resulting logits tensor.

b) Cross-entropy loss prediction

For target tokens $Y \in \{1, 2, \dots, V\}^{B \times T}$, the loss is:

$$\mathcal{L} = -\frac{1}{BT} \sum_{b=1}^B \sum_{t=1}^T \log \frac{\exp(Z_{b,t,Y_{b,t}})}{\sum_{v=1}^V \exp(Z_{b,t,v})} \quad (2)$$

This formulation requires full materialization of Z , which scales as $O(B \cdot T \cdot V)$. For large vocabularies, this tensor dominates GPU memory and bandwidth usage, even though only one logit per position ($Z_{b,t,Y_{b,t}}$) is ultimately consumed.

3.2 Proposed Approach

Our key insight is that the cross-entropy loss can be computed directly from hidden states and target tokens without explicitly forming the full logits tensor. Specifically:

$$\mathcal{L} = -\frac{1}{BT} \sum_{b=1}^B \sum_{t=1}^T (H_{b,t} \cdot W_{Y_{b,t}}^T - \log \sum_{v=1}^V \exp(H_{b,t} \cdot W_v^T)) \quad (3)$$

- $H_{b,t} \cdot W_{Y_{b,t}}^T$ computes only the logit corresponding to the target token at position (b, t)
- The dominator term is evaluated via a streaming reduction, avoiding storage of all intermediate logits

This fused formulation eliminates the need to materialize Z , reducing memory footprint from $O(B \cdot T \cdot V)$ to $O(B \cdot T)$, while maintaining the exact equivalence to the standard two-stage pipeline.

To ensure numerical stability while avoiding full logits materialization, our fused kernel employs a streaming variant of the softmax computation. Instead of storing all vocabulary logits, the algorithm maintains two running variables per position: the current maximum logit and an accumulator of exponentials relative to that maximum. As each vocabulary entry is processed, the maximum and accumulator are updated simultaneously, guaranteeing stability against overflow or underflow. The target logit corresponding to the ground-truth token is tracked separately for the numerator, while the denominator is reconstructed at the end as the product of the maximum's exponential and the accumulated sum. This design allows the loss to be computed exactly as in the standard cross-entropy formulation, but without ever instantiating the full $(B \cdot T \cdot V)$ logits tensor. By combining projection and loss computation in a single pass, the algorithm reduces memory footprint, alleviates bandwidth pressure, and preserves correctness under safe softmax semantics. Algorithm 1 details the implementation of the fused kernel.

Algorithm 1 Fused Output Projection and Cross-Entropy Prediction with Safe Softmax

Require: Hidden states $H \in \mathbb{R}^{B \times T \times d}$, Output weights $W \in \mathbb{R}^{V \times d}$, Target tokens $Y \in \{1, \dots, V\}^{B \times T}$

Ensure: Cross-entropy loss \mathcal{L}

- 1: Initialize $\mathcal{L} \leftarrow 0$
- 2: **for** $b = 1$ to B **do**
- 3: **for** $t = 1$ to T **do**
- 4: Initialize $m \leftarrow -\infty$ {running maximum}
- 5: Initialize $a \leftarrow 0$ {accumulated sum}
- 6: Initialize $z_{\text{target}} \leftarrow 0$
- 7: **for** $v = 1$ to V **do**
- 8: Compute logit: $z \leftarrow H_{b,t} \cdot W_v^\top$
- 9: **if** $z > m$ **then**
- 10: $a \leftarrow a \cdot \exp(m - z) + 1$
- 11: $m \leftarrow z$
- 12: **else**
- 13: $a \leftarrow a + \exp(z - m)$
- 14: **end if**
- 15: **if** $v = Y_{b,t}$ **then**
- 16: $z_{\text{target}} \leftarrow z$
- 17: **end if**
- 18: **end for**
- 19: Compute denominator: $s \leftarrow \exp(m) \cdot a$
- 20: Update loss: $\mathcal{L} \leftarrow \mathcal{L} - \log \frac{\exp(z_{\text{target}})}{s}$
- 21: **end for**
- 22: **end for**
- 23: Normalize: $\mathcal{L} \leftarrow \mathcal{L} / (B \cdot T)$
- 24: **return** \mathcal{L}

For clarity of presentation, we detail the forward algorithm here, while the backward pass is described separately in Appendix A.1.

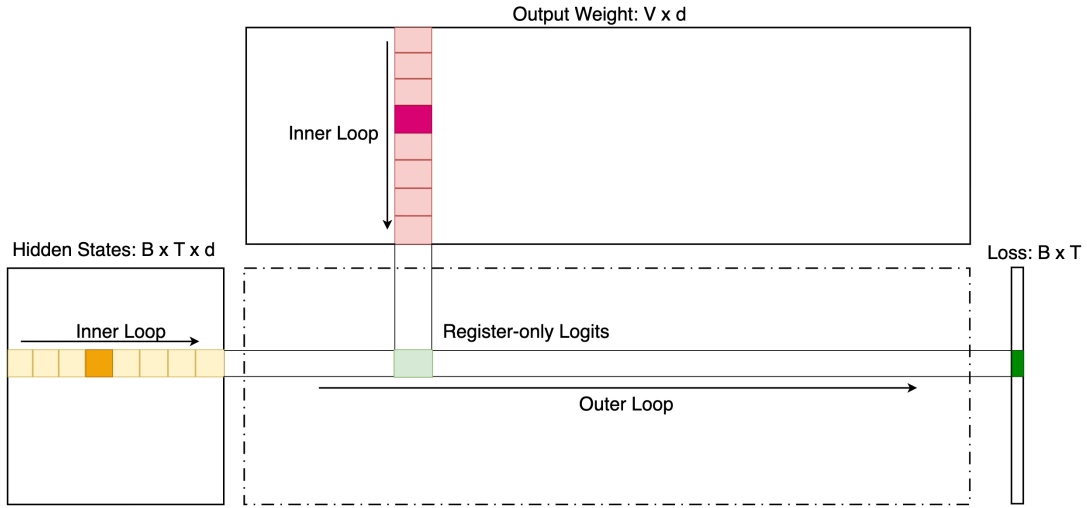


Figure 1: GPU-friendly forward pass with register-level logits and parallel accumulation updates

To visually illustrate the projection-prediction fusion, Figure 1 depicts the key computation steps in the forward pass. Yellow tiles represent slices of the hidden state tensor, while pink

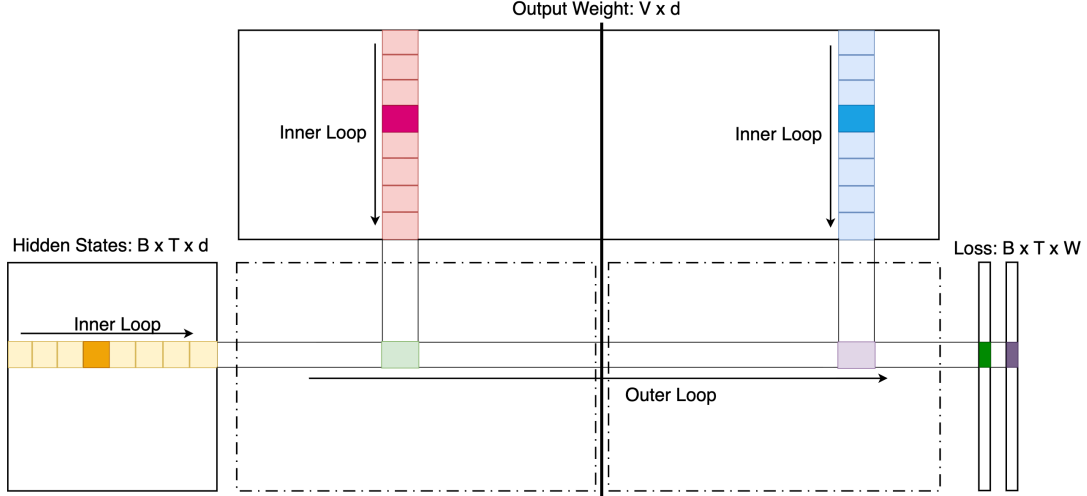


Figure 2: Window-based forward pass with parallel accumulation updates

tiles denote segments of the output weight matrix assigned to each thread block. The diagram emphasizes the nested loop structure of the output layer: the inner loop performs dot products between hidden states and output weights, and the outer loop accumulates contributions across the vocabulary dimension. This tile-based execution enables parallel updates to the running maximum and normalization accumulator, two critical components of the numerically stable softmax. The design is well-suited to GPU architecture, leveraging warp-level parallelism and register-local reductions. The intermediate logits tensor is shown as a dashed box, indicating that it is never materialized in device memory but instead computed and consumed on-the-fly within GPU registers.

3.2.1 Window-based Strategy

In the vanilla design, each thread block performs accumulation across the vocabulary dimension in parallel for a given (b, t) position. While this approach is effective when the product $B \times T$ is large, it suffers from poor GPU occupancy when $B \times T$ is small - particularly in scenarios with a large vocabulary size V , where the number of active blocks becomes insufficient to saturate the device.

To mitigate this limitation, we introduce a tunable hyperparameter called the *window size*, denoted by W , which partitions the outer loop into multiple chunks. Each window is processed independently by a group of blocks, enabling finer-grained parallelism and better utilization of GPU resources. Figure 2 illustrates this window-based strategy for enhancing occupancy during the forward pass. The diagram shows two distinct windows, each representing a chunk of the outer loop split along the vocabulary axis. By assigning separate groups of thread blocks to process each window independently, this design increases parallel granularity and ensures high GPU utilization even when $B \times T$ is small. This approach allows concurrent accumulation across the vocabulary dimension within each window, improving throughput without altering the computational semantics.

In order to obtain final prediction result, an additional epilogue operation is required to aggregate the partial outputs from all windows.

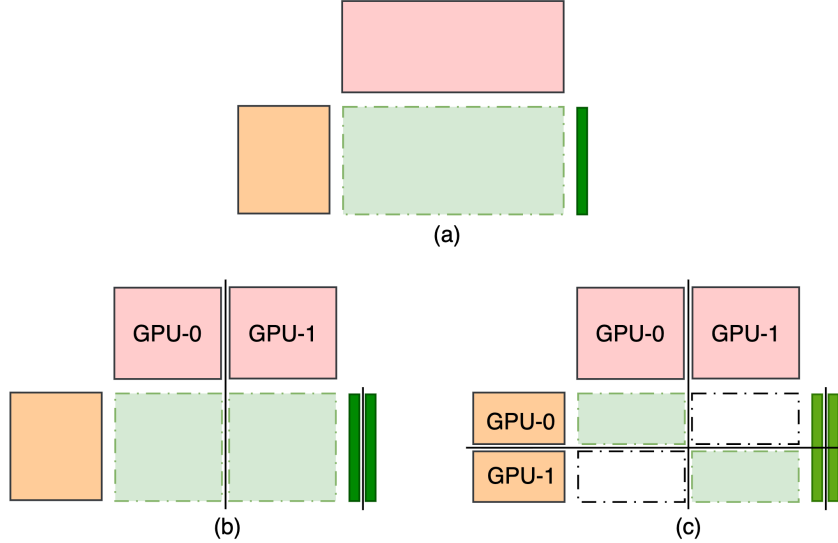


Figure 3: Model parallelism patterns

3.2.2 Model Parallelism

The proposed method is readily extensible to support a variety of model parallelism strategies [19]. Among the most commonly adopted patterns in large-scale language model training are Data Parallelism (DP), Tensor Parallelism (TP), and Sequence Parallelism (SP), each targeting different bottlenecks in memory and compute distribution.

Figure 3 illustrates how our work integrates with these parallelism schemes. In this figure, yellow boxes represent hidden states, pink boxes denote output weights, light green boxes indicate register-only logits, and dark green boxes correspond to the final loss predictions.

1. Data Parallelism, Figure 3(a)

In DP, each GPU processes a distinct mini-batch of input data while maintaining a full copy of the model parameters, including hidden states and output weights. Gradients are computed independently on each device and synchronized across ranks during the backward pass. This strategy is widely adopted due to its simplicity and scalability. Our fused kernels integrate seamlessly into this setup, requiring no changes to the DP workflow.

2. Tensor Parallelism, Figure 3(b)

TP partitions the output weight matrix along the vocabulary axis across GPU ranks. Each rank computes logits and partial predictions for its assigned vocabulary shard. Our fused kernel supports this configuration by restricting the outer loop to the local weight slice and accumulating partial results accordingly. To produce the final prediction, partial outputs must be aggregated across all TP ranks.

3. Sequence Parallelism, Figure 3(c)

SP further divides the hidden states along the sequence axis, typically layered on top of TP. Each GPU processes a subset of the sequence positions while retaining a shard of the output weights. Our design accommodates this setup by first gathering partial hidden states and then convert the SP layout into a TP-compatible pattern. This ensures that all SP ranks produce consistent prediction results without introducing semantic divergence.

4 Experiments

To evaluate the effectiveness of the proposed projection-prediction combination method, we conduct a series of experiments measuring both runtime performance and memory consumption. Our goal is to quantify the benefits of eliminating the logits materialization and leveraging register-local computation, particularly in regimes where vocabulary size and sequence length pose scalability challenges.

4.1 Experimental Setup

We implement these kernels with NVIDIA CUTEDSL [20] and OpenAI Triton [21], and incorporate them into the PyTorch-based training pipeline. To verify its effectiveness, we compare it against the canonical two-stage implementation that separately computes logits and applies cross-entropy loss [9]. All experiments are conducted on NVIDIA GB200 GPU with 186GB memory, using mixed-precision training (BF16). We benchmark across multiple batch sizes, sequence lengths, and vocabulary sizes to capture a range of realistic training scenarios.

Table 1 summarizes the experimental settings.

Table 1: Experimental setup

Aspect	Config
Data Type	BF16
GPU	NVIDIA GB200
PyTorch	2.9.0
OpenAI Triton	3.4.0
NVIDIA CUTEDSL	4.2.1
Hidden Dimension, d	4096
Range of $B \times T$	1024,4096,8192,16384,32768
Range of V	32768,65536,131072,262144
Model Parallelism	Data Parallelism

Since the input datatype is BF16 [22], intermediate logits must be upcast to FP32 [23] during computation to safeguard against numerical underflow and overflow. In the canonical two-stage approach, this upcasting occurs within the GEMM operation, where the full logits tensor is materialized in device memory. In contrast, our method inherently avoids this overhead by performing the upcast within register-local computation.

4.2 Results

Table 2 presents a comprehensive comparison between the canonical and proposed method across varying vocabulary size V and batch-sequence products $B \times T$ under Data Parallelism. Figure 4 visualizes the latency trends, while Figure 5 illustrates memory usage. Together, these results demonstrate that our proposed method consistently outperforms the canonical two-stage implementation in both runtime and memory efficiency.

Latency, measured in milliseconds, increases with vocabulary size due to the growing cost of output projection and loss computation. This trend holds across all $B \times T$ configurations. However, our kernel significantly mitigates this growth. For instance, at $B \times T = 32,768$ and $V = 262,144$, the canonical method incurs a latency of 96.42 ms, whereas our method reduces

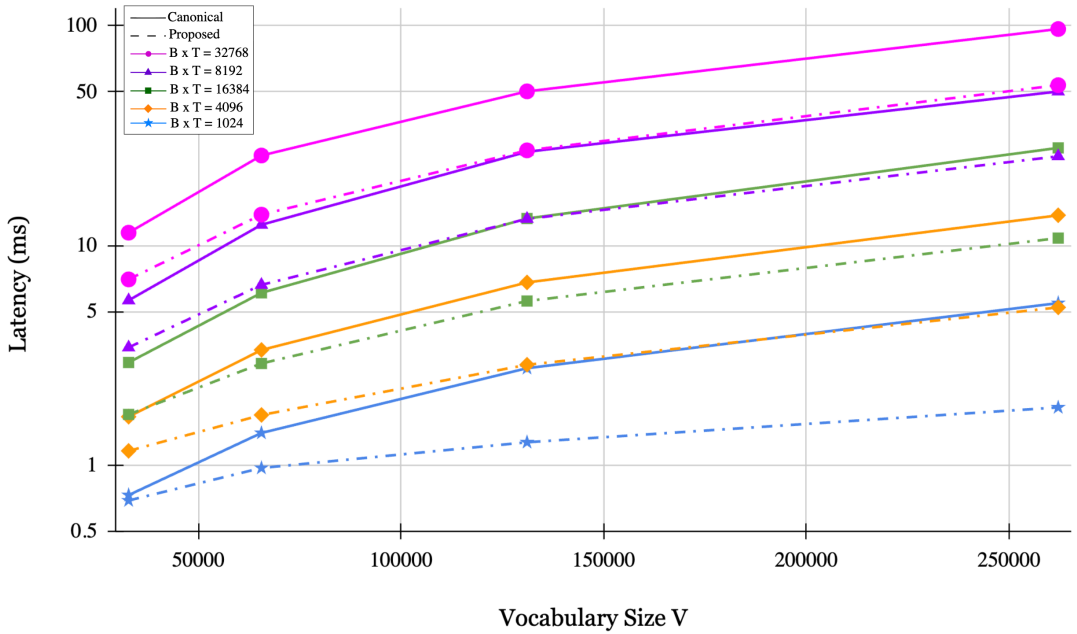


Figure 4: Latency Comparison between Canonical and Proposed Methods. The lower, the better.

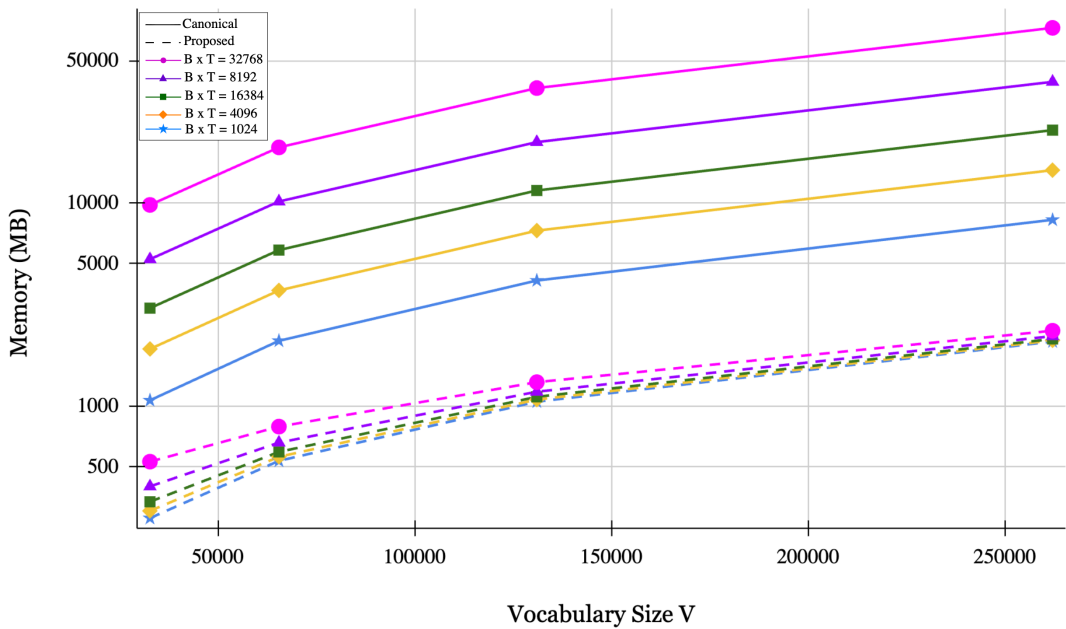


Figure 5: Memory Comparison between Canonical and Proposed Methods. The lower, the better.

Table 2: Latency (ms) and memory usage (MB) comparison between canonical and proposed methods across varying $B \times T$ and vocabulary sizes V on Data-Parallelism. The lower, the better.

$B \times T$	V	Latency (ms)		Memory (MB)	
		Canonical	Proposed	Canonical	Proposed
1024	32,768	0.73	0.69	1064	280
	65,536	1.40	0.97	2088	536
	131,072	2.76	1.27	4136	1048
	262,144	5.46	1.83	8232	2072
4096	32,768	1.66	1.16	1904	304
	65,536	3.34	1.69	3696	561
	131,072	6.78	2.86	7280	1073
	262,144	13.70	5.22	14448	2099
8192	32,768	2.93	1.70	3024	337
	65,536	6.08	2.90	5840	593
	131,072	13.25	5.58	11472	1107
	262,144	27.77	10.79	22736	2133
16384	32,768	5.62	3.43	5264	401
	65,536	12.41	6.61	10128	659
	131,072	26.67	13.20	19856	1173
	262,144	50.15	25.43	39312	2203
32768	32,768	11.42	7.00	9744	531
	65,536	25.64	13.80	18704	790
	131,072	50.24	27.06	36624	1307
	262,144	96.52	53.61	72464	2342

it to 53.61 ms - yielding a **44.5%** improvement. Figure 4 illustrates this pattern, showing that the proposed method maintains a consistently lower latency curve across all vocabulary sizes.

Memory usage, gauged in megabytes, also scales linearly with vocabulary size in the canonical implementation due to full logits tensor materialization. In contrast, our method avoids this overhead by computing logits in a register-local fashion. As shown in Table 2, the memory savings are substantial. At $B \times T = 32,768$ and $V = 262,144$, the canonical method consumes 72.5 GB, while our method requires only 2.3 GB - a reduction of over **96.8%**. Figure 5 highlights this efficiency, with the proposed method exhibiting a much flatter memory growth curve.

Across all tested configurations, the proposed method delivers consistent improvements in both latency and memory footprint. These gains become increasingly pronounced at larger vocabulary sizes and longer sequence lengths, making our approach particularly well-suited for scaling LLM training in memory-constrained or latency-sensitive environments.

5 Discussion

The experimental results confirm that our fused projection-prediction kernel consistently outperforms the canonical two-stage implementation in both latency and memory usage across diverse vocabulary sizes and sequence configurations. These improvements are most pronounced in

large-scale settings, where the cost of output projection and logits materialization emerges as a dominant bottleneck.

The performance improvements arise from collapsing the boundary between the projection and loss stages. By fusing these operations, the proposed method achieves finer-grained GPU resource utilization and better overlap between CUDA Core and Tensor Core execution. This design reduces kernel launch overhead, increases arithmetic intensity, and ultimately delivers higher throughput. Furthermore, by eliminating the need to materialize the full logits tensor in device memory, our method alleviates bandwidth pressure and avoids costly I/O associated with reading and writing large activation tensors.

In the canonical approach, a large intermediate logits tensor must be stored, scaling with $B \times T \times V$ and imposing significant memory and bandwidth demands. Our method sidesteps this by computing logits on-the-fly within register-local scopes, enabling execution with a lower memory footprint and reduced data movement. This design aligns naturally with the architectural strengths of modern GPUs, which favor compute-bound workloads with minimized memory traffic. The result is a streamlined execution pipeline that scales gracefully with vocabulary size.

While the fused kernel offers clear advantages, it introduces additional complexity in kernel design and debugging. Numerical stability must be carefully managed, particularly under mixed-precision regimes (e.g., BF16 inputs with FP32 accumulation), where rounding behavior can affect convergence. Moreover, although the NVIDIA CUDA toolkit provides the flexibility required for fine-grained register control and efficient tensor core scheduling, the fusion strategy may be less portable to programming environments - such as OpenAI Triton - that abstract away low-level resource management. These are not hardware limitations, but software constraints imposed by higher-level compilation frameworks.

Although our experiments focus on the standard cross-entropy loss, the proposed combining method is not restricted to this objective. By collapsing the boundary between projection and prediction, the fused design generalizes naturally to more complex output layers, including multi-task heads, structured prediction objectives, and loss variants such as label smoothing or sampled softmax. In all these cases, the principle of avoiding logits materialization and leveraging register-local computation applies, enabling efficient scaling without fundamental redesign. This extensibility underscores the broader applicability of our approach beyond standard training setups.

Future work will extend the fusion strategy to support additional loss functions such as label smoothing and sampled softmax. Our current implementation already supports tensor parallelism and sequence parallelism; ongoing experiments will further validate its effectiveness and scalability in multi-GPU and multi-node environments. Another promising direction is automated kernel generation using compiler-based approaches, specifically within the NVIDIA CUDA ecosystem. Rather than targeting cross-architecture portability, we aim to deepen optimization within NVIDIA’s GPU stack, reducing manual kernel engineering while preserving fine-grained control over register usage and tensor core scheduling.

6 Conclusion

Training large language models at scale is increasingly constrained by the cost of output projection and loss computation, particularly as vocabulary sizes and sequence lengths grow. The canonical two-stage approach suffers from high latency and excessive memory usage due to the materialization of large logits tensors, creating a bottleneck in both performance and scalability.

To address this challenge, we proposed a fused projection-prediction kernel that collapses the boundary between projection and loss computation. By computing logits on-the-fly within register-local scopes, our method eliminates the need to store intermediate tensors, reduces memory bandwidth pressure, and enables finer-grained utilization of GPU resources. This design achieves better overlap between CUDA Core and Tensor Core execution, improving arithmetic intensity and throughput.

Experimental results demonstrate that the proposed method consistently outperforms the canonical implementation across a wide range of vocabulary sizes and batch-sequence configurations. At large scales, the improvements are particularly striking: latency reductions of over 40% and memory savings exceeding 95% were observed. These gains highlight the effectiveness of our approach in mitigating the dominant bottlenecks of LLM training.

Beyond cross-entropy loss, the fused design generalizes naturally to more complex objectives, including multi-task heads, structured prediction, and loss variants such as label smoothing or sampled softmax. This extensibility underscores the broader applicability of our method across diverse training regimes.

Looking ahead, future work will focus on further validating the integration of our fused kernel with tensor and sequence parallelism to assess scalability in multi-GPU and multi-node environments. We also see compiler-assisted kernel generation - within the NVIDIA CUDA ecosystem - as a promising direction to automate and extend the fusion strategy across diverse model architectures and training regimes. Rather than pursuing cross-platform generalization, our goal is to deepen optimization within NVIDIA’s software stack, reducing engineering overhead while preserving fine-grained control. Ultimately, our approach contributes to more efficient and scalable training pipelines, supporting the continued evolution of large language models under increasingly demanding computational constraints.

Acknowledgments

We would like to thank NVIDIA DevTech team for valuable comments and suggestions.

References

- [1] Zihao Yi, Jiarui Ouyang, Zhe Xu, Yuwen Liu, Tianhao Liao, Haohao Luo, and Ying Shen. A survey on recent advances in llm-based multi-turn dialogue systems, 2025. URL <https://arxiv.org/abs/2402.18013>.
- [2] Leonid Legashev, Alexander Shukhman, Vadim Badikov, and Vladislav Kurynov. Using large language models for goal-oriented dialogue systems. *Applied Sciences*, 15(9):4687, 2025. doi: <https://doi.org/10.3390/app15094687>.
- [3] Stefano Bistarelli, Marco Fiore, Ivan Mercanti, and Marina Mongiello. Usage of large language model for code generation tasks: A review. *SN Computer Science*, 6(673), 2025. doi: <https://doi.org/10.1007/s42979-025-04241-5>.
- [4] Yanbo Zhang, Sumeer A. Khan, Adnan Mahmud, Huck Yang, Alexander Lavin, Michael Levin, Jeremy Frey, Jared Dunnmon, James Evans, Alan Bundy, Saso DZeroski, Jesper Tegner, and Hector Zenil. Exploring the role of large language models in the scientific method: from hypothesis to discovery. *NPJ Artificial Intelligence*, 1(14), 2025. doi: <https://doi.org/10.1038/s44387-025-00019-5>.

[5] Tian Jin, Nolan Clement, Xin Dong, Vaishnavh Nagarajan, Michael Carbin, Jonathan Ragan-Kelley, and Gintare Karolina Dziugaite. The cost of scaling down large language models: Reducing model size affects memory before in-context learning. In *ICLR 2024*. ICLR Proceedings, 2024.

[6] Julian Büchel, Aristotelis Vasilopoulos, Werner A. Simon, and et al. Efficient scaling of large language models with mixture of experts and 3d analog in-memory computing. *Nature Computational Science*, 5:13–26, 2025. doi: 10.1038/s43588-024-00753-x.

[7] M. Ahmad, A.A. Abdulkadhem, U. Islam, et al. Optimizing large language models in distributed environments: A holistic approach to efficiency, ethics, and governance. *International Journal of Computational Intelligence Systems*, 18:293, 2025. doi: 10.1007/s44196-025-00992-4.

[8] Chaofan Tao, Qian Liu, Longxu Dou, Niklas Muennighoff, Zhongwei Wan, Ping Luo, Min Lin, and Ngain Wong. Scaling laws with vocabulary: Larger models deserve larger vocabularies, 2024. URL <https://arxiv.org/html/2407.13623v1>.

[9] Fan Yuantao, Li Ruifan, Zhang Guangwei, Shi Chuan, and Wang Xiaojie. A weighted cross-entropy loss for mitigating llm hallucinations in cross-lingual continual pretraining. In *ICASSP 2025 - 2025 IEEE International Conference on Acoustics, Speech and Signal Processing (ICASSP)*, pages 1–5, 2025. doi: 10.1109/ICASSP49660.2025.10888877.

[10] Taeho Kim, Yanming Wang, Vatshank Chaturvedi, Lokesh Gupta, Seyeon Kim, Yongin kWon, and Sangtae Ha. Llmem: Estimating gpu memory usage for fine-tuning pre-trained llms. In *IJCAI 2024*, 2024. URL <https://www.ijcai.org/proceedings/2024/0699.pdf>.

[11] Maxim Milakov and Natalia Gimelshein. Online normalizer calculation for softmax, 2018. URL <https://arxiv.org/pdf/1805.02867>.

[12] Dao Tri, Fu Daniel Y., Ermon Stefano, Rudra Atri, and Ré Christopher. FlashAttention: Fast and memory-efficient exact attention with IO-awareness. In *Advances in Neural Information Processing Systems (NeurIPS)*, 2022.

[13] Dao Tri. FlashAttention-2: Faster attention with better parallelism and work partitioning. In *International Conference on Learning Representations (ICLR)*, 2024.

[14] Samyam Rajbhandari, Jeff Rasley, Olatunji Ruwase, and Yuxiong He. Zero: Memory optimizations toward training trillion parameter models, 2020. URL <https://arxiv.org/abs/1910.02054>.

[15] Samyam Rajbhandari, Olatunji Ruwase, Jeff Rasley, Shaden Smith, and Yuxiong He. Zero-infinity: Breaking the gpu memory wall for extreme scale deep learning, 2021. URL <https://arxiv.org/abs/2104.07857>.

[16] Budiman Setiawan, Rochimah Siti, and Siahaan Daniel O. The survey of model scale impact on knowledge distillation efficiency in llm. In *2025 International Electronics Symposium (IES)*, pages 771–776, 2025. doi: 10.1109/IES67184.2025.11161662.

[17] Ashish Vaswani, Noam Shazeer, Niki Parmar, Jakob Uszkoreit, Llion Jones, Aidan N. Gomez, Lukasz Kaiser, and Illia Polosukhin. Attention is all you need, 2023. URL <https://arxiv.org/abs/1706.03762>.

[18] NVIDIA. Transformerengine. <https://github.com/NVIDIA/TransformerEngine>, 2025.

- [19] Mohammad Shoeybi, Mostafa Patwary, Raul Puri, Patrick LeGresley, Jared Casper, and Bryan Catanzaro. Megatron-lm: Training multi-billion parameter language models using model parallelism, 2020. URL <https://arxiv.org/abs/1909.08053>.
- [20] NVIDIA. Domain specific language for cute, 2025. URL https://docs.nvidia.com/cutlass/latest/media/docs/pythonDSL/quick_start.html.
- [21] OpenAI. Triton: Open-source gpu programming for neural networks, 2021. URL <https://openai.com/index/triton/>.
- [22] NVIDIA. Bf16 data type, 2020. URL <https://images.nvidia.com/aem-dam/en-zz/Solutions/data-center/nvidia-ampere-architecture-whitepaper.pdf>.
- [23] IEEE. Ieee standard for floating-point arithmetic. *IEEE Std 754-2019 (Revision of IEEE 754-2008)*, pages 1–84, 2019. doi: 10.1109/IEEESTD.2019.8766229.

A Appendix

A.1 Backward Pass

For each position (b, t) , let $z_v = H_{b,t} \cdot W_v^T$ and $P_v = \frac{\exp(z_v)}{\sum_{v=1}^V \exp(z_v)}$. The cross-entropy gradient w.r.t. logits is $\frac{\partial L}{\partial z_v} = P_v - 1[v == Y_{b,t}]$. In the fused setup, we obtain P_v via the same streaming, numerically stable softmax used in the forward pass: maintain the running maximum m and accumulator a , then compute $P_v = \exp(z_v - m)/a$ on the fly for each v . Gradients propagate without materializing the logits tensor,

the gradient w.r.t. hidden states is

$$\frac{\partial L}{\partial H_{b,t}} = \sum_{v=1}^V \frac{\partial L}{\partial z_v} \cdot W_v = \sum_{v=1}^V (P_v - 1[v == Y_{b,t}]) \cdot W_v \quad (4)$$

and the gradient w.r.t. output weights accumulates as

$$\frac{\partial L}{\partial W_v} = \sum_{b=1}^B \sum_{t=1}^T \frac{\partial L}{\partial z_v} \cdot H_{b,t} = \sum_{b=1}^B \sum_{t=1}^T (P_v - 1[v == Y_{b,t}]) \cdot H_{b,t} \quad (5)$$

Operationally, the kernel streams over v , to re-compute forward logit z_v and then compute P_v stably using (m, a) , updates $\partial L / \partial H_{b,t}$ by accumulating $(P_v - 1[v == Y_{b,t}])W_v$, and atomically accumulates $\partial L / \partial W_v$ with $(P_v - 1[v == Y_{b,t}])H_{b,t}$. This preserves exact gradients while avoiding storage of $Z \in R^{B \cdot T \cdot V}$.

Algorithm 2 details the implementation of the backward pass.

Algorithm 2 Backward Pass with Logit Recompute and Safe Softmax

Require: Hidden states H , Output weights W , Targets Y , Safe-softmax stats (m, a) from forward, Upstream gradient Γ (e.g., $\Gamma = 1/(B \cdot T)$ for mean reduction)

Ensure: Gradients $\partial H, \partial W$

- 1: Initialize $\partial H \leftarrow 0, \partial W \leftarrow 0$
- 2: **for** $b = 1$ to B **do**
- 3: **for** $t = 1$ to T **do**
- 4: $\partial H_{b,t} \leftarrow 0$
- 5: **for** $v = 1$ to V **do**
- 6: $z \leftarrow H_{b,t} \cdot W_v^\top$
- 7: $p_v \leftarrow \exp(z - m)/a$
- 8: $g_v \leftarrow \Gamma_{b,t} \cdot (p_v - \mathbf{1}[v = Y_{b,t}])$
- 9: $\partial H_{b,t} \leftarrow \partial H_{b,t} + g_v \cdot W_v$
- 10: $\partial W_v \leftarrow \partial W_v + g_v \cdot H_{b,t}$
- 11: **end for**
- 12: **end for**
- 13: **end for**
- 14: **return** $\partial H, \partial W$

Furthermore, there exists a more radical strategy to achieve the same objective. In this variant, the training pipeline is restructured to perform **partial gradient accumulation** for both hidden states and output weights directly within the forward pass. The subsequent backward pass then applies the upstream gradient to rescale these partial results, producing the final gradients. By design, this approach eliminates the need to recompute the logits during backpropagation and thereby avoids redundant matrix multiplications, substantially reducing computational overhead. **It is important to note, however, that this method is only applicable when the upstream gradient is a scalar - namely, when the loss reduction mode is set to either mean or sum.**

Algorithm 3 presents the forward pass with integrated partial gradient accumulation, while Algorithm 4 illustrates the subsequent backward scaling step that incorporates the upstream gradient.

Algorithm 3 Forward with Safe Softmax + Partial Gradient Accumulation

Require: $H \in \mathbb{R}^{B \times T \times d}$, $W \in \mathbb{R}^{V \times d}$, $Y \in \{1, \dots, V\}^{B \times T}$

Ensure: Loss \mathcal{L} , partial grads $\partial' H$, $\partial' W$; cached stats (m, a)

- 1: $\mathcal{L} \leftarrow 0$, $\partial' H \leftarrow 0$, $\partial' W \leftarrow 0$
- 2: **for** $b = 1$ to B **do**
- 3: **for** $t = 1$ to T **do**
- 4: $m \leftarrow -\infty$, $a \leftarrow 0$, $z_{\text{target}} \leftarrow 0$
- 5: **for** $v = 1$ to V **do**
- 6: $z \leftarrow H_{b,t} \cdot W_v^\top$
- 7: **if** $z > m$ **then**
- 8: $a \leftarrow a \cdot \exp(m - z) + 1$; $m \leftarrow z$
- 9: **else**
- 10: $a \leftarrow a + \exp(z - m)$
- 11: **end if**
- 12: **if** $v = Y_{b,t}$ **then**
- 13: $z_{\text{target}} \leftarrow z$
- 14: **end if**
- 15: **end for**
- 16: $s \leftarrow \exp(m) \cdot a$
- 17: $\mathcal{L} \leftarrow \mathcal{L} - \log(\exp(z_{\text{target}})/s)$
- 18: **Partial gradient accumulation (unscaled by upstream)**
- 19: $\partial' H_{b,t} \leftarrow 0$
- 20: **for** $v = 1$ to V **do**
- 21: $z \leftarrow H_{b,t} \cdot W_v^\top$ {recompute or cache per-tile}
- 22: $p_v \leftarrow \exp(z - m)/a$
- 23: $g'_v \leftarrow p_v - \mathbf{1}[v = Y_{b,t}]$
- 24: $\partial' H_{b,t} \leftarrow \partial' H_{b,t} + g'_v \cdot W_v$
- 25: $\partial' W_v \leftarrow \partial' W_v + g'_v \cdot H_{b,t}$
- 26: **end for**
- 27: Cache (m, a) (optional if recomputing in backward is cheap)
- 28: **end for**
- 29: **end for**
- 30: **return** $\mathcal{L}, \partial' H, \partial' W, (m, a)$

Algorithm 4 Backward Scaling with Upstream Gradient

Require: Partial gradients $\partial' H$, $\partial' W$; upstream gradient Γ

Ensure: Final gradients ∂H , ∂W

```
1: if  $\Gamma$  is scalar then
2:    $\partial H \leftarrow \Gamma \cdot \partial' H$ 
3:    $\partial W \leftarrow \Gamma \cdot \partial' W$ 
4: else
5:   Initialize  $\partial H \leftarrow 0$ ,  $\partial W \leftarrow 0$ 
6:   for  $b = 1$  to  $B$  do
7:     for  $t = 1$  to  $T$  do
8:        $\alpha \leftarrow \Gamma_{b,t}$ 
9:        $\partial H_{b,t} \leftarrow \alpha \cdot \partial' H_{b,t}$ 
10:      Note: For weights, either store per-position contributions  $\partial' W^{(b,t)}$  in forward,
11:          then compute  $\partial W \leftarrow \sum_{b,t} \alpha \cdot \partial' W^{(b,t)}$  here.
12:     end for
13:   end for
14: end if
15: return  $\partial H, \partial W$ 
```
